

# CNN-based Dual-Chain Models for Knowledge Graph Learning

Bo Peng · Renqiang Min · Xia Ning

Received: date / Accepted: date

**Abstract** Knowledge graph learning plays a critical role in integrating domain-specific knowledge bases when deploying machine learning and data mining models in practice. Existing methods on knowledge graph learning primarily focus on modeling the relations among entities as translations among the relations and entities, and many of these methods are not able to handle zero-shot problems, when new entities emerge. In this paper, we present a new convolutional neural network (CNN)-based dual-chain model. Different from translation based methods, in our model, interactions among relations and entities are directly captured via CNN over their embeddings. Moreover, a secondary chain of learning is conducted simultaneously to incorporate additional information and to enable better performance. We also present an extension of this model, which incorporates descriptions of entities and learns a second set of entity embeddings from the descriptions. As a result, the extended model is able to effectively handle zero-shot problems. We conducted comprehensive experiments, comparing our methods with 15 methods on 8 benchmark datasets. Extensive experimental results demonstrate that our proposed methods achieve or outperform the state-of-the-art results on knowledge graph learning, and outperform other methods on zero-shot problems. In addition, our methods applied to real-world biomedical data are able to produce results that conform to expert domain knowledge.

---

B.Peng  
The Ohio State University  
E-mail: peng.707@buckeyemail.osu.edu

R. Min  
NEC Laboratories America, Inc.  
E-mail: renqiang@nec-labs.com

X. Ning  
The Ohio State University  
E-mail: ning.104@osu.edu

## 1 Introduction

Real-world knowledge can be represented in directed, multi-relational, and structured graphs, the so-called knowledge graphs. In a knowledge graph, graph nodes represent entities of interest and edges encode relations among entities. Therefore, one piece of knowledge can be succinctly represented by two nodes and one edge between them in the knowledge graph, where the source node is referred to *head* and the destination node is referred to *tail*. Thus, the whole collection of such (head, relation, tail) triplets captures entirely the knowledge graph structure and content. Real-world knowledge graphs include WordNet [15], a large lexical database for English, Google Knowledge Graph <sup>1</sup>, a comprehensive system about facts among people, etc., and DBpedia [10], a structured knowledge base for information extracted from Wikipedia, etc.

Typically, knowledge graphs suffer from incompleteness, that is, many relations (i.e., edges) among entities (i.e., nodes) in the graphs cannot be established due to the limited or unknown information. It is substantially significant to enable complete knowledge graphs. For example, a complete knowledge graph on the relations between diseases and genes, and the relations between genes and drugs, could dramatically help improve medicine and health care. However, knowledge graph completion, and in general, knowledge graph learning, is a very challenging task, requiring strong modeling power to capture the underlying logic that governs the formation of the head-relation-tail triplets, and thus, the knowledge.

Substantial research efforts have been dedicated to knowledge graph learning, in particular, from the deep learning community, due to the extraordinary capability of deep learning in modeling complicated relations among data. Quite a few deep learning methods [2, 4, 7, 8, 11, 21, 22, 25] (Section 2) have been developed and have dramatically improved knowledge graph learning. Still, there exist increasing needs to further improve knowledge graph learning performance, particularly for high-impact applications such as medicine and health care. In addition, being able to leverage additional information from other sources, for example, descriptions on entities, to improve knowledge graph learning, is very promising but less explored.

In this paper, we present our efforts toward improving knowledge graph learning as follows:

- We present new deep learning methods, termed as Convolutional Neural Network (CNN)-based Dual-Chain methods, denoted as **CDC**, for knowledge graph learning. Very different from existing methods (Section 2), **CDC** models the interactions among relations and entities via a CNN over their respective embeddings as features for the corresponding triplet. Then, logistic regression is used to predict whether the triplets are valid from the learned features.
- In addition to the above primary learning process, we introduced a secondary chain of simultaneous learning process in **CDC**, which learns from sparsified entity and relation embeddings in a same architecture as in the primary chain. This dual-chain structure in **CDC** helps reduce overfitting, accelerate convergence and improve learning performance in general.
- We also developed an extension of **CDC**, denoted as **CDG+**, to incorporate and utilize textual information (i.e., entity descriptions) in knowledge graph learning.

---

<sup>1</sup> <https://developers.google.com/knowledge-graph/>

In **CDG $\dagger$** , entities and relations will both have a second embedding learned from the descriptions via structure attention and CNNs. The embeddings learned from graph structures (i.e., the head-relation-tail triplets) and from the descriptions are used together along the dual chains to enable more accurate prediction on triplets. Thus, **CDG $\dagger$**  is able to improve learning performance and handle zero-shot problems [24].

- We conducted comprehensive experiments on 8 public, benchmark datasets, and compared our methods with another 15 methods on knowledge graph learning. The experimental results demonstrate that our methods are able to achieve or outperform the state of the art.
- We also investigated our methods on two important biological knowledge graphs: drug-gene interaction graph and drug-drug interaction graph. Our experimental results demonstrate that our methods outperform the state-of-the-art knowledge graph learning methods, and make discoveries supported by expert domain knowledge.

Table 1 presents the key definitions and notations used in this paper. The rest of this paper is organized as follows. Section 2 presents the related work. Section 3 presents the details of **CDC** method. Section 4 presents the details of **CDG $\dagger$**  method. Section 5 compares **CDC** with existing methods. Section 6 presents the experimental protocols, datasets and evaluation metrics. Section 7 presents the experimental results. In Section 8, we conclude our work and discuss future work.

Table 1: Definitions and Notations

notation	meaning
$e/E$	entity/entity set
$r/R$	relation/relation set
$h/t$	head/tail entity
$(h, r, t)$	a head-relation-tail triplet
$S/S'$	set of positive/negative $(h, r, t)$ triplets
$v/v^s$	embedding/sparsified embedding of size $k$

## 2 Related Work

In this section, we review the literature on knowledge graph learning, particularly using deep neural networks, based on how the relations among entities are formulated and learned, and which information is used to learn the relations.

### 2.1 Translation based Knowledge Graph Learning

The most popular way to formulate the relations among entities in knowledge graph learning is through translation, pioneered by the work of Bordes *et al.* [2] on the TransE method. In TransE, a true relation  $r$  between head  $h$  and tail  $t$  is represented as a linear translation among their respective embeddings  $v_r$ ,  $v_h$  and  $v_t$ , that is,  $v_h + v_r = v_t$ . Thus, a false relation  $r'$  between head  $h'$  and tail  $t'$  will induce a large distance between  $v_h + v_r$  and  $v_t$ . All the entity and relation embeddings are learned via optimizing a pairwise ranking objective among all the triplets, that is, distances from positive triplets are smaller than the distances

from their corresponding negative triplets. Wang *et al.* [22] developed TransH, which also uses the linear translation as in TransE to model relations. Different from TransE, in TransH, one hyperplane is learned for each relation. Head and tail entities are projected onto the hyperplane of a relation as relation-specific embeddings. The linear translation is done on the hyperplane to predict if the relation holds for the projected heads and tails. TransR [11] is another translation based method. In TransR, entities and relations are represented in two different spaces. For each relation, a mapping function is learned to map the head and tail entities from the entity space to the relation space, where the relations between the head and tail entities are represented via the translation as in TransE. Cluster-based TransR (CTransR) [11] is an extension of TransR. In CTransR, the triplets of a same relation are clustered into groups. In each group, a relation embedding is learned, as well as a cluster-specific mapping function that maps entities into the relation space. Thus, in CTransR, a relation will have multiple embeddings and multiple mapping functions so as to capture the different subtypes among a same relation. The translation among entities is same as that in TransR in the relation space.

Existing work also tackles the mapping functions to embed entities and relations within the translation based learning framework. In TransD [7], a dynamic mapping matrix is calculated from the embeddings of entities and relations to map entities from entity space to relation space. In the relation space, a translation as in TransE is used to model the relations among entities. TranSparse [8] uses relation-specific sparse mapping matrices to map entities into the relation space, similarly as in TransR and TransD. The sparsity of the mapping matrices varies according to the complexity of the relations. Thus, complexities among the relations can be captured via mapping matrix sparsity, and meanwhile, overfitting risks are decreased. DistMult [25] represents relations using diagonal matrices (e.g.,  $W_r$ ) and use a bilinear scoring function to measure the distance from  $h$  through  $r$  to  $t$  (e.g.,  $hW_r t^\top$ ). In ComplEx [21], the distance from  $h$  through  $r$  to  $t$  is also measured by dot product. However, instead of using a single representation for the entities and relations, ComplEx learns multiple representations for each entity and relation in different domains. The distances from  $h$  through  $r$  to  $t$  in the different domains are then combined (multiplied) as the final distance. HolE [16] can be considered as a special case of ComplEx, which models relations between entities using compositional vector representations based on circular correlations. In ConvE [4], a 2D CNN architecture is used to convert  $v_h$  and  $v_r$  to an estimated  $\tilde{v}_t$ . The similarity between  $\tilde{v}_t$  and the true tail embedding  $v_t$ , via dot product, is used to calculate the probability score of  $(h, r, t)$ . Different from these methods mainly based on simple linear translations or correlations between (transformed) embeddings, our proposed methods learn a powerful nonlinear scoring metric of the  $(h, r, t)$  triplets, and directly model complex interactions between relation and entity embeddings via a CNN.

## 2.2 Knowledge Graph Learning with Additional Information

Existing work also incorporates additional information (e.g., textual information of entities, paths in knowledge graphs) to improve performance on knowledge graph learning. DKRL [24] incorporates entity descriptions in words, and applies a 2-

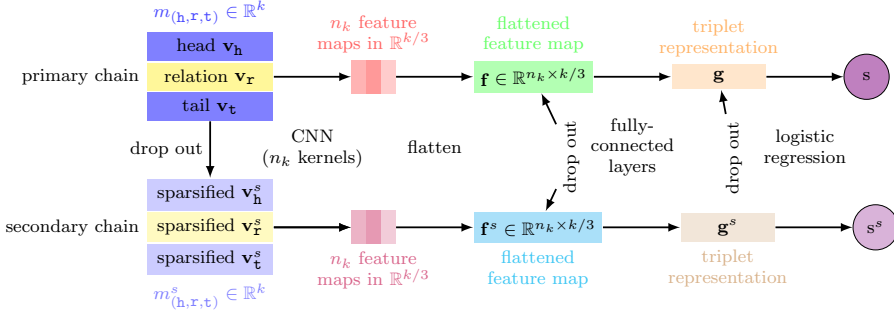


Fig. 1: CDC Model Architecture

layer CNN to map word descriptions to entity embeddings, in addition to learning another set of entity and relation embeddings from the  $(\mathbf{h}, \mathbf{r}, \mathbf{t})$  triplets (i.e., knowledge graph structure). DKRL leverages the translation idea from TransE, and enforces small distances between  $\mathbf{v}_h + \mathbf{v}_r$  and  $\mathbf{v}_t$  for all positive triplets, using the embeddings learned from both word descriptions and knowledge graph structures. With the entity descriptions, DKRL is able to calculate embeddings for entities that are not in its training data, and thus handle the zero-shot problem [24]. CBOW [24] is a variation of DKRL, in which the descriptions are represented using the bag-of-word representation by their top-20 words weighted by TF-IDF. R-GCN [19] incorporates the path information of knowledge graphs. R-GCN learns the embedding for each entity in the knowledge graph via graph convolution [17], and uses a similar idea as in DistMult to measure the relation between head and tail entities (i.e., dot product between head embedding, diagonal matrix of relation and tail embedding). SSP [23] learns a topic model of the textual descriptions of entities. Unlike these previous approaches, our methods model entity descriptions with CNNs over word embeddings enhanced with a structural attention mechanism and perform knowledge graph completion in our proposed CNN based triplet scoring framework.

### 3 CNN-based Dual-Chain Model (CDC)

We develop a novel CNN-based Dual-Chain model, denoted as CDC, for entity and relation prediction in knowledge graph. CDC has two chains of learning processes: a primary chain and a secondary chain. In the primary chain of learning processes, each entity  $\mathbf{e} \in \mathcal{E}$  and each relation  $\mathbf{r} \in \mathcal{R}$  will be embedded into a low-dimensional vector  $\mathbf{v}_e \in \mathbb{R}^k$  and  $\mathbf{v}_r \in \mathbb{R}^k$ , respectively, in a same latent space, where  $k$  is the embedding dimension. A CNN will be applied on the entity and relation embeddings so as to capture their interactions, which will be used to predict  $(\mathbf{h}, \mathbf{r}, \mathbf{t})$  triplets. We will learn such embeddings via supervised learning in CDC such that true (positive)  $(\mathbf{h}, \mathbf{r}, \mathbf{t})$  triplets will be scored high and false (negative) triplets will be scored low. A secondary chain of learning processes is designed to relax the primary learning process so as to avoid overfitting, and meanwhile to strengthen the major signals that will be learned from the primary chain in order to enforce robust and consistent predictions. Figure 1 presents the architecture of CDC.

### 3.1 CDC Model Architecture

#### 3.1.1 Dual Embedding Representations

In CDC, given a triplet  $(h, r, t)$ , we stack their embedding vectors  $v_h$ ,  $v_r$  and  $v_t$  into a matrix  $m_{(h,r,t)} \in \mathbb{R}^{3 \times k}$ , that is,  $m_{(h,r,t)} = [v_h; v_r; v_t]$ . Meanwhile, we also use a sparsified version of  $m_{(h,r,t)}$ , denoted as  $m_{(h,r,t)}^s$ , by randomly dropping out 20% of values in  $m_{(h,r,t)}$ . Both of  $m_{(h,r,t)}$  and  $m_{(h,r,t)}^s$  will go through exactly same network architectures with same parameters, and will be learned with shared parameters in almost identical ways (except drop-out operations as indicated in Figure 1). Therefore, we only discuss the learning for  $m_{(h,r,t)}$  in the following section. The process with  $m_{(h,r,t)}/m_{(h,r,t)}^s$  as input is referred to as the primary/secondary chain, respectively.

The use of the sparsified embeddings in addition to the original embeddings is inspired by ComplEx [21], which learns multiple embeddings for each entity to capture different aspects of the entity information. In our experiments, we observed that learning multiple embeddings to represent each entity (i.e, replacing  $m_{(h,r,t)}^s$  by another embedding that is also learned from the  $(h, r, t)$  triplet) will induce overfitting. Instead, we use the sparsified version  $m_{(h,r,t)}^s$  as a second representation for  $(h, r, t)$ . Thus, the secondary chain is expected to still capture the major signals learned in  $m_{(h,r,t)}$  and strengthen such signals as  $m_{(h,r,t)}^s$  goes through almost same learning process as  $m_{(h,r,t)}$  with same model parameters. Meanwhile, the learning for the model parameters will be regularized by the drop-out operations along the chains, thus the risk of overfitting is reduced. The other drop-outs as in Figure 1 will be discussed in Section 3.1.2.

#### 3.1.2 Convolution and Feature Mapping

We first use  $n_c$  kernels of size  $3 \times 3$  to conduct convolution over  $m_{(h,r,t)}$  (and same for  $m_{(h,r,t)}^s$ ). The convolution will go through the rows of  $m_{(h,r,t)}$  as indicated in Figure 2. Therefore, it will capture the interactions between  $h$ ,  $r$  and  $t$  since the kernels have same height as  $m_{(h,r,t)}$  and thus cover and integrate information from  $h$ ,  $r$  and  $t$  at the same time. It is expected that the interaction patterns among positive triplets are different from those among negative triplets, and thus lead to different label predictions. Out of the convolution, we will produce  $n_k$  feature maps of size  $k/3 \times 1$ . We apply ReLU activation function, defined as  $\text{ReLU}(x) = \max(0, x)$ , on each of feature maps to generate non-negative feature maps. The ReLU activation is used here to only keep the non-negative interactions among the triplets that will contribute to their labels, and meanwhile introduces non-linearity in the feature mapping.

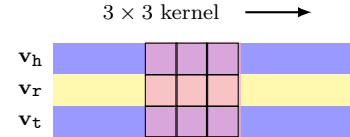


Fig. 2: CDC Convolution over Triplet Matrix

After the convolution operation, we flatten the feature maps (i.e., the output of the convolution operation) into a feature vector  $\mathbf{f}$  of size  $1 \times (n_k k/3)$  with 20% of the values randomly dropped out. We use a fully-connected layer (i.e., a projection matrix) with ReLU activation function and map  $\mathbf{f}$  into another low-dimension feature  $\mathbf{g}$  as in Equation 1,

$$\mathbf{g} = f(\mathbf{f} \mathbf{W}_f + \mathbf{b}_f), \quad (1)$$

where  $\mathbf{W}_f$  and  $\mathbf{b}_f$  are the projection matrix and the bias,  $f()$  is the ReLU function. After the mapping,  $\mathbf{g}$  will have 20% of its values randomly dropped out. The embedding  $\mathbf{m}_{(h,r,t)}^s$  will go through exactly the same operations with same parameters, except that drop-out is only applied on the flattened feature maps. The resulted feature from the fully-connected layer is denoted as  $\mathbf{g}^s$ . Please note that the two drop-outs in the primary chain are to prevent overfitting along the primary chain. In the secondary chain, since the input triplets are already sparsified, we only applied drop-out on the flattened feature maps, not on the triplet representations. Our experiments showed that without any drop-outs on the secondary chain, the performance is suboptimal compared to one drop-out on the secondary chain.

### 3.1.3 Logistic Regression

We consider the feature  $\mathbf{g}$  out of the fully-connected layer as the feature representation of the triplet. In **CDC**, a positive triplet should be assigned a high score and a negative triplet should have a low score. We use logistic regression to calculate the scores for the triplets based on  $\mathbf{g}$ . The scoring function on  $\mathbf{g}$  is as in Equation 2,

$$s(h, r, t) = \sigma(\mathbf{g} \mathbf{W}_l + \mathbf{b}_l) = \sigma(f(\mathbf{f} \mathbf{W}_f + \mathbf{b}_f) \mathbf{W}_l + \mathbf{b}_l), \quad (2)$$

where  $\sigma$  is the sigmoid function,  $\mathbf{W}_l$  and  $\mathbf{b}_l$  are the linear mapping weights and bias. Similarly, for  $\mathbf{m}_{(h,r,t)}^s$ , the score out of logistic regression is denoted as  $s^s$ . Both  $s$  and  $s^s$  will be optimized as described in Section 3.2 in order to learn the model.

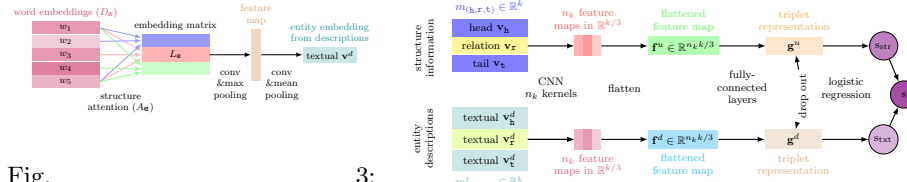


Fig.

3:

Entity Embeddings from Descriptions in DFG. 4: CDC+ Model Architecture

### 3.2 The CDC Optimization Problem

We use entropy loss as the objective in order to learn the **CDC** model. As mentioned in Section 3.1.3 and shown in Figure 1, **CDC** will produce two scores  $s$  and  $s^s$  for each

triplet. During training, we optimize these two scores jointly. Thus, the objective function for **CDC** is as in Equation 3,

$$\min_{\Theta} \sum_{(h, r, t) \in S} \log(s(h, r, t)) + \sum_{(h', r', t') \in S'} \log(1 - s(h', r', t')) + \\ \sum_{(h, r, t) \in S} \log(s^s(h, r, t)) + \sum_{(h', r', t') \in S'} \log(1 - s^s(h', r', t')), \quad (3)$$

where  $\Theta = \{\mathbf{m}_{(h, r, t)}, \mathbf{b}_f, \mathbf{W}_f, \mathbf{b}_l, \mathbf{W}_l, \mathcal{K}\}$  is the set of parameters in **CDC** and  $\mathcal{K}$  is the set of kernels used for convolution,  $S$  is the set of positive triplets and  $S'$  is manually corrupted negative set as will be described in Section 3.3, and  $s$  and  $s^s$  are defined as in Equation 2. That is, **CDC** makes predictions from two input embeddings, and optimizes both of the two predicted scores to be close to the ground truth. The score  $s$  is used to predict the relations among triplets during testing.

The reason why only  $s$ , instead of both  $s$  and  $s^s$ , is used for prediction is that, when testing, the drop-out rate will be 0. As a result, the secondary chain will also start from the same entity and relation embeddings as in the primary chain. Since the architectures of the two chains are identical,  $s$  and  $s^s$  calculated from the two chains will be identical. For simplicity, we use  $s$  for prediction in **CDC**. However, during model learning, both  $s$  and  $s^s$  are used in the objective function so  $s^s$  can enhance  $s$  for better optimization. We also observed from our experiments that the performance without  $s^s$  in the objective function is worse than that with both the scores. The reason why we use entropy loss instead of pairwise ranking loss is that we observed tie problems from pairwise ranking loss in our experiments, that is, multiple triplets may have exactly same scores and thus be ranked equally, which causes overestimate using ranking based metric (e.g., hits at 10 as will be discussed in Section 6.2).

### 3.3 CDC Learning Algorithm and Negative Triplet Generation

We initialize the embeddings and the model parameters using uniform distributions over  $[-\sqrt{\frac{6}{n_{in}+n_{out}}}, \sqrt{\frac{6}{n_{in}+n_{out}}}]$  [5], where  $n_{in}$  is the in dimension,  $n_{out}$  is the out dimension of the embeddings or parameters (e.g., for a matrix  $X \in \mathbb{R}^{m \times n}$ ,  $m$  is the in dimension,  $n$  is the out dimension). At each epoch, multiple batches are created and used as training data, and mini-batch stochastic gradient descent method is used to update all the parameters. The training batches are generated as follows. We first randomly choose  $n_b$  positive triplets from positive training set  $S$ . For every positive triplet  $(h, r, t)$ , we generate a corresponding negative triplet by randomly replacing either  $h$  or  $t$  (but not both at same time) by  $h'$  or  $t'$ , where  $(h', r, t) \notin S$  and  $(h, r, t') \notin S$ . The negative triplets are sampled for each batch of positive triplets. We use the distribution described in Wang *et al.* [22] to decide to replace head or tail. Therefore, there will be  $n_b$  pairs of positive and negative triplets in a batch. We use the batches of  $n_b$  pairs of triplets for **CDC** model learning.

#### 4 CDG+ with Entity Descriptions

When entity descriptions are available, they may provide additional, useful information that can help relation prediction over entities. Thus, we extend **CDC** to incorporate available entity descriptions, and denote the new model as **CDG+**. Given the entity descriptions in the form of word vectors, **CDG+** learns a mapping function from entity descriptions to entity embeddings. Figure 3 presents the scheme of such mapping. Structure attention mechanism [12] and two-layers CNN [24] are applied to learn the entity embeddings from descriptions, denoted as  $\mathbf{v}^d$ .

##### 4.1 Attention and Convolution over Word Embeddings

We use the structure attention mechanism [12] to map the word embeddings of the descriptions of an entity, denoted as  $D_e$ , to a more expressive embedding matrix denoted as  $L_e$ . The attention weights are calculated from  $D_e$  as follows,

$$A_e = \text{softmax}(V \tanh(UD_e^\top)), \quad (4)$$

where  $U$  and  $V$  are two weighting matrices shared across all the entities.  $A_e$  is the attention weight matrix, which maps  $D_e$  to  $L_e$  as follows,

$$L_e = A_e D_e. \quad (5)$$

Intuitively, each row of  $L_e$  represents one semantic aspect of the entity  $e$ 's description.

We use a two-layer CNN to map the  $L_e$  to an entity embedding  $\mathbf{v}^d$ . In the first layer, a convolution kernel is applied on  $L_e$ , followed by a max pooling. The output from this layer goes through a second layer of convolution, followed by a mean pooling. The output will be reshaped into  $\mathbf{v}_e^t$  for the entity  $e$ .

##### 4.2 Learning with Entity Descriptions

Given the descriptions, we are able to produce two heterogeneous embeddings for each entity. One is from the structure information (i.e., relations among entities) and the other is from the textual information (i.e., entity descriptions in words). We use the architecture shown in Figure 4 to calculate two scores  $s_{\text{str}}$  and  $s_{\text{txt}}$  from these two embeddings, respectively, and use the mean of these two scores as the output from the architecture. This method is denoted as **CDG+**. That is, **CDG+** replaces the sparsified version of the entity embeddings in **CDC** (Figure 1) in the inputs by the entity description embeddings (Figure 3), and the two scores at the output in **CDC** by the mean of two scores. Also, **CDG+** applies drop-outs over the triplet representations, with all the other architectures in **CDC** remained same. The reason why the mean of  $s_{\text{str}}$  and  $s_{\text{txt}}$  is used as the output is that we consider the embeddings from the entity descriptions and knowledge graph structure information both important in contributing to the final prediction, as they may encode different, complementary information about the entities.

In **CDG+**, we denote the triplet representations (similar as  $\mathbf{g}$  and  $\mathbf{g}^s$  in **CDC**) learned from structure information and textual information as  $\mathbf{g}^u$  and  $\mathbf{g}^d$ , respectively. We enforce the similarity between  $\mathbf{g}^u$  and  $\mathbf{g}^d$  by introducing an  $\ell_1$ -norm

penalty in **CDG+** model training so that the structure information and the textual information can be better fused in the model. We use  $\ell_1$  norm here due to its empirical superior performance over other norms (e.g.,  $\ell_2$  norm) in similar applications [24]. Therefore, the objective function for **CDG+** is as follows,

$$\begin{aligned} \min_{\Theta} \quad & \sum_{(h, r, t) \in S} \log(s(h, r, t)) + \sum_{(h', r', t') \in S'} \log(1 - s(h', r', t')) \\ & + \sum_{S \cup S'} \|\mathbf{g}^d - \mathbf{g}^u\|_{\ell_1}, \\ \text{s.t.,} \quad & s(h, r, t) = 0.5 \times (s_{\text{txt}}(h, r, t) + s_{\text{str}}(h, r, t)), \\ & s(h', r', t') = 0.5 \times (s_{\text{txt}}(h', r', t') + s_{\text{str}}(h', r', t')), \end{aligned} \quad (6)$$

where  $\Theta = \{U, V, D_e, \Theta_{\text{CNN}}, \mathbf{m}_{(h, r, t)}, \mathbf{b}_f, W_f, \mathbf{b}_l, W_l, \mathcal{K}\}$ , where  $\Theta_{\text{CNN}}$  is the set of parameters of the two-layer CNN including the kernels and bias, and  $\mathcal{K}$  is the set of kernels as in **CDC**. The learning algorithm for **CDG+** is same to that for **CDC** as in Section 3.3.

## 5 Comparison between CDC and Existing Methods

The model that is most similar to **CDC** is ConvE [4], which employs 2D CNNs to learn embeddings for entities and relations. However, there are several key differences between **CDC** and ConvE. The ConvE model architecture is shown in Figure 5 (extracted from the ConvE paper [4]).

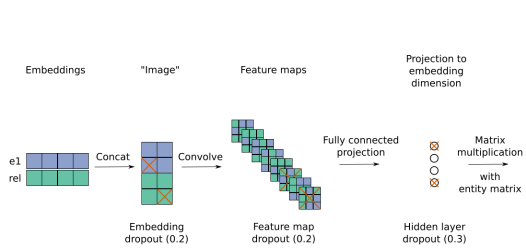


Fig. 5: ConvE Model Architecture

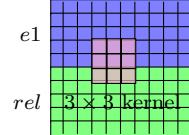


Fig. 6: ConvE Convolution over Head and Relation Embeddings

In ConvE, the embedding of head (e.g.,  $e1$  in Figure 5) and relation (e.g.,  $rel$  in Figure 5) are stacked and reshaped into a matrix (e.g., of size  $10 \times 20$ , the matrix under ‘‘Image’’ in Figure 5), denoted as  $e1$  and  $rel$  respectively. Then, a CNN along with a fully-connected layer is employed to project the head and relation representations together into an embedding (e.g., the embedding under ‘‘Projection to embedding dimension’’ in Figure 5). The probabilities of the projected embedding belonging to different tail entities are calculated via the dot product between the projected embedding and the corresponding entity embeddings and logits (e.g., the probabilities under ‘‘Predictions’’ in Figure 5). The key idea of ConvE is similar to TransE [2], that is, to ‘‘translate’’ head and relation to tail, except that ConvE uses a CNN rather than a simple linear operation as in TransE to model the translation. In ConvE, multiple kernels are used in the CNN to capture the interactions

between head and relation. However, the kernels are typically very small (e.g.,  $3 \times 3$  for  $10 \times 20$  reshaped matrices). Therefore, the kernels can only capture the interactions at the boundaries of the head and relation embeddings as demonstrated in Figure 6. However, in **CDC**, the CNN can directly capture the interactions from the entirety of the head, relation and tail embeddings as demonstrated in Figure 2.

## 6 Experimental Protocols

### 6.1 Datasets and Comparison Methods

We use the following 8 public datasets in our experiments: Yago3-10 [14], WN18 [2], FB15k [2], FB14k [24], FB15k-237 [4], FB20k [24], DGI [3] and DDI [20].

- *YAGO3-10 dataset* contains relations among people and their attributes (e.g., (“Alex”, “is a”, “football player”)), and each relation has more than 10 triplets.
- *WN18* is a subset of WordNet [15]. Most triplets in WN18 represent the semantic relation between words.
- *FB15k dataset* is a subset of Freebase [1]. Most triplets record facts about actors, awards, sports, sport teams and movies, and their relations.
- *FB14k dataset* is a subset of FB15k, with entities that do not have descriptions removed.
- *FB15k-237 dataset* is another subset of FB15k, where inverse relations are removed.
- *FB20k dataset* is an extension of FB14k. It contains 19,923 entities, among which 5,019 entities never appear in the training set.
- *DGI dataset* is a subset of drug-gene interaction dataset described in Cotto *et al.* [3] with interaction types of frequency higher than 50. Common drug-gene interaction types include activation and inhibition, etc.
- *DDI dataset* is a subset of drug-drug interaction dataset TWOSIDES [20] with interaction types of frequency between 500 and 1,100. Relations in DDI represent side effects that are induced by drug-drug interactions. Common drug-drug interaction (i.e., side effect) types include food intolerance, breast cyst and bunion, etc.

The first 6 datasets are widely used benchmark datasets in knowledge graph learning. The last 2 datasets are biological datasets for important biological problems. It’s noteworthy that FB15k and WN18 are reported to have test leakage issues [4]. Although FB15k and WN18 are widely used, they may not be good benchmarks for the evaluation purpose. Table 2 presents the statistics of the datasets.

We compare **CDC** with the following 15 methods in total, where the results of these methods on the datasets are available from literature: TransE [2], TransH [22], TransR [11], CTransR [11], KG2E [6], TransD [7], TranSparse [8], HolE [16], Dist-Mult [25], ComplEx [21], R-GCN [19]. We did not compare with ConvE due to the data unfairness and reproducibility issues as discussed later in Appendix A.1. We include the corresponding results in Table 10 in appendix. We compare **CDC** with DKRL [24] and SSR [23], which are able to use entity descriptions and have results reported on FB14k.

Table 2: Dataset Statistics

dataset	#entity	#relation	#train	#valid	#test
YAGO3-10	123,182	37	1,079,040	5,000	5,000
WN18	40,943	18	141,442	5,000	5,000
FB15k	14,951	1,345	483,142	50,000	59,071
FB14k	14,904	1,341	472,860	48,991	57,809
FB15k-237	14,541	237	272,115	17,535	20,466
FB20k	19,923	1,341	472,860	48,991	30,490
DGI	7,217	14	15,781	1,130	1,131
DDI	538	25	20,951	2,618	2,617

The columns corresponding to #entity, #relation, #train, #valid and #test have the number of entities, the number of relations, the number of training, validation and testing triplets, respectively.

## 6.2 Evaluation Metrics

We use two popular evaluation metrics: mean rank (MR) [2] and hits at 10 (H@10) [2], to evaluate the performance of the methods, calculated as follows. For each positive triplet in the testing set, we generate a set of negative triplets by corrupting its head by each of the other entities in E, but remove the negative triplets if they are in training or validation set. We predict the scores for each positive triplet and its corresponding negative triplets, and rank all the triplets using their predicted scores in descending order. MR is calculated as the average ranking position of all the positive testing triplets among their corresponding negative triplets. Low MR indicates that true positive triplets are ranked high, and thus good performance. H@10 is calculated as the fraction of the positive testing triplets over all positive testing triplets that are ranked into top 10 among their corresponding negative testing triplets. High H@10 indicates that many true positive triplets are ranked among top 10 of their negative triplets, and thus good performance.

## 7 Experimental Results

### 7.1 Entity Prediction

For all the testing triplets ( $h, r, t$ ), we conducted two sets of experiments: 1) prediction of  $t$  given  $h$  and  $r$ , and 2) prediction of  $h$  given  $t$  and  $r$ . We evaluated the performance of each experiment using MR and H@10, and present the respective average results over the two sets of the experiments in Table 3, 4 and 5.

Table 3 presents the comparison between CDC and another 10 state-of-the-art methods on WN18 and FB15k datasets. The results of the other 10 methods are cited from their respective publications. On WN18, CDC achieves the best H@10 (94.9%), tied with HolE. In terms of MR CDC is not as good as many of the others. This indicates that CDC is able to rank the majority positive testing triplets very high among top 10, but a small portion of the positive testing triplets lower than other methods. However, given the large number of entities in WN18 (i.e., 41k as in Table 2), we consider the performance of CDC in terms of MR is still reasonable (i.e.,  $1-380/40,943=99.07\%$ ile). On FB15k, CDC is the 2nd best method in terms of MR (73), slightly worse than that of KG2E (MR = 59). In

Table 3: Entity Prediction on WN18 and FB15k

method	WN18		FB15k	
	MR	H@10	MR	H@10
TransE [2]	251	89.2	125	47.1
TransH [22]	303	86.7	87	64.4
TransR [11]	225	92.0	77	68.7
CTransR [11]	218	92.3	75	70.2
KG2E [6]	331	92.8	<b>59</b>	70.4
TransD [7]	212	92.2	91	77.3
TranSparse [8]	<b>211</b>	93.2	82	79.5
DistMult [25]	-	93.6	-	82.4
ComplEx [21]	-	94.7	-	<b>84.0</b>
Hole [16]	-	<b>94.9</b>	-	73.9
<b>CDC</b>	380	<b>94.9</b>	73	83.3

The best performance under each metric is **bold**. H@10 values are in percent.

terms of H@10, **CDC** is the 2nd best method (H@10 = 83.3%), only very slightly worse than ComplEx (H@10 = 84.0%). We believe H@10 is more meaningful in real applications when only a top few predictions will be further investigated, and when it is very costly to validate every one in the top, for example, 211 predictions (TranSparse’s MR = 211). Thus, **CDC** achieves the state-of-the-art performance in terms of H@10 on WN18 and FB15k, and comparable performance on MR, compared with the other methods. Note that we also conducted experiments in which only the primary chain in **CDC** is used and the secondary chain is removed. However, the performance of this simplified **CDC** is worse than **CDC**. For example, on FB15k, this method achieves H@10 = 79.0%, compared to that of **CDC** (83.3%). Thus, we did not present such results in the tables. Please also note that, although we present the experimental results on FB15k and WN18 as they are widely used benchmarks, these two datasets may not properly evaluate the methods due to their serious test leakage issue as reported in [4]. In order to further evaluate our method, we conduct experiments on more difficult datasets, in which the interactions among triplets are more complicated.

Table 4: Entity Prediction on YAGO3-10 and FB15k-237

method	YAGO3-10		FB15k-237	
	MR	H@10	MR	H@10
DistMult [25]	5,926	54.0	<b>254</b>	41.9
ComplEx [21]	6,351	55.0	339	42.8
R-GCN [19]	-	-	-	41.7
<b>CDC</b>	<b>2,061</b>	<b>62.9</b>	267	<b>46.2</b>

The best performance under each metric is **bold**. H@10 values are in percent.

Table 4 presents the comparison between **CDC** and 3 state-of-the-art methods on YAGO3-10 and FB15k-237 datasets. The results of the 3 methods are cited from [4]. Other methods do not have results reported on these two datasets. On YAGO3-10, **CDC** achieves the best H@10 (62.9%) and MR among all the methods. On FB15k-237, **CDC** also achieves the best H@10 and MR. Thus, based on both Table 3 and Table 4, **CDC** performs better than the other comparison methods on average.

The state-of-the-art performance and significant improvement on these difficult datasets properly demonstrate the strong ability of **CDC** in modeling interactions among triplets.

Table 5: Entity Prediction on DDI and DGI

method	DGI		DDI	
	MR	H@10	MR	H@10
DistMult [25]	157	86.6	66	22.0
ComplEx [21]	174	<b>87.3</b>	64	31.6
<b>CDC</b>	<b>88</b>	86.8	<b>35</b>	<b>35.7</b>

The best performance under each metric is **bold**. H@10 values are in percent.

Table 5 presents the comparison between **CDC**, DistMult and ComplEx. On DGI, **CDC** achieves the best MR (88) compared to DistMult and ComplEx, and the 2nd best H@10 (86.8%), which is slightly worse than ComplEx’s. On DDI, **CDC** achieves the best MR and H@10 compared to DistMult and ComplEx, and the improvement over ComplEx, the 2nd best method, is very significant (i.e., 45% in MR and 13% in H@10).

## 7.2 Entity Prediction with Descriptions

### 7.2.1 Entity Prediction from Structure and Textual Information

We use FB14k to evaluate the performance of **CDG+**. FB14k is a benchmark dataset to evaluate knowledge graph learning with descriptions [24]. The statistics of FB14k is presented in Table 2.

In **CDG+**, we use Glove [18] pre-trained 100-dimension word vectors to initialize the embeddings for each word in the entity descriptions. For each entity, we use the first 200 words in its description with necessary padding, since 99.2% entities have descriptions of fewer than 200 words. We compared **CDG+** with DKRL [24] and SSP [23] as they reported the state-of-the-art performance on FB14k. For DKRL, when both the entity embeddings from structure information and from entity descriptions are used in prediction, DKRL is denoted as DKRL (ALL). When only the entity descriptions are used, the method is denoted as DKRL (CNN). For SSP, when the knowledge graph learning model and the topic model are trained separately, SSP is denoted as SSP (Std.). When the tow models are trained simultaneously, it is denoted as SSP (Joint).

We conduct three sets of experiments on **CDG+**, following the experimental setting of Xie *et al.* [24]. In the first experiment, we use the mean of the  $s_{txt}$  and  $s_{str}$  as the predicted score, as exactly in **CDG+**. In the second experiment, we only use  $s_{str}$  in **CDG+**, not  $s_{txt}$ , as the predicted score. This method is denoted as **CDG+ (str)**. In the third experiment, we only use  $s_{txt}$  in **CDG+**, not  $s_{str}$ , as the predicted score. This method is denoted as **CDG+ (txt)**. Table 6 presents the experimental results from all the comparison methods on FB14k.

Table 6 demonstrates that **CDG+** achieves the best H@10 (84.5%) among all the methods. **CDG+ (txt)** achieves the second best H@10 (84.1%) and **CDG+ (str)** achieves a

Table 6: Entity Prediction with Descriptions on FB14k

method	MR	H@10
DKRL (CNN) [24]	113	57.6
DKRL (ALL) [24]	91	67.4
SSP (Std.) [23]	<b>77</b>	78.6
SSP (Joint) [23]	82	79.0
CDC	109	82.7
CDC+(str)	101	75.7
CDC+(txt)	107	84.1
<b>CDC+</b>	109	<b>84.5</b>

CDC+(str) and CDC+(txt) represent that in CDC+, only  $s_{str}$  or  $s_{txt}$  is used for prediction, respectively. The best performance under each metric is **bold**. H@10 values are in percent.

poor H@10 (75.7%), even worse than that from CDC (82.7%) when no textual information is used. Both CDC+(txt) and CDC+(str) train a CDC+ model but use different scores for prediction. The good performance of CDC+(txt) indicates that textual information is useful in entity prediction, while the worse performance of CDC+(str) than CDC demonstrates the effectiveness of the dual-chain architecture in CDC (i.e., only structure information is used in the model) in improving performance and reducing overfitting. The fact that CDC+ outperforms both CDC+(txt) and CDC+(str) indicates that the structure and textual information might be complementary and combining them will benefit entity prediction. The fact that CDC+ outperforms CDC indicates the capability of CDC+ in integrating structure information and textual information for entity prediction.

### 7.2.2 Zero-Shot Learning

Most traditional knowledge graph methods can not handle new entities that are not involved in the knowledge graph during training. Our CDC+ provides a natural way to deal with this zero-shot problem by learning entity representations through their textual descriptions, and using the scores predicted from the textual information (i.e.,  $s_{str}$  in CDC+) for prediction (i.e., CDC+(txt) as in Table 6). We compare CDC+ with another two methods CBOW [24] and DKRL [24], which are able to deal with zero-shot learning. We test these methods on dataset FB20k [24], in which each testing triplet has at least one new entity. In our experiments, the testing set is split into 3 subsets with different types of triplets: 1). triplets with new entities at head, denoted as N-h; 2). triplets with new entities at tail, denoted as N-t; and 3). triplets with new entities at both heads and tails, denoted as N-ht. Table 7 presents the FB20K data statistics on N-h, N-t and N-ht.

Table 7: Statistics of FB20k

dataset	#entity	#N-h	#N-t	#N-ht	#total
FB20k	19,923	18,753	11,586	151	30,490

We test CDC+, CBOW and DKRL on these three subsets and present the results in Table 8. We use the CDC+ model that is trained from FB14k and performs best

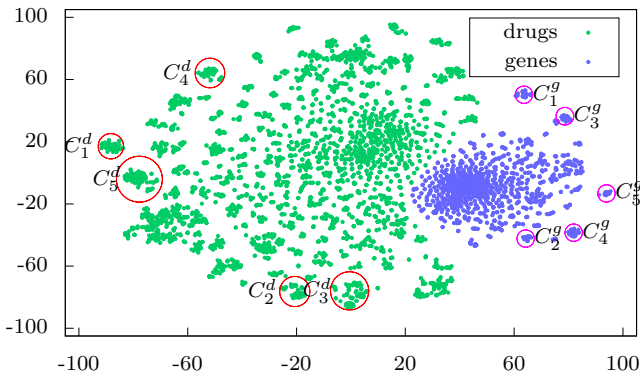
on FB14k to test FB20k, following the setting in [24]. Our results demonstrate that **CDG+(txt)** substantially outperforms CBOW and DKRL on **N-h** and **N-t**. In particular, **CDG+(txt)** outperforms DKRL (the second best method) 30.7% and 40.2% on **N-h** and **N-t**, respectively. On **N-ht**, **CDG+(txt)** is slightly worse than DKRL (CNN) but still 3.9% better than CBOW. However, given the very limited size of **N-ht**, the slight difference between **CDG+(txt)** and DKRL (CNN) (i.e., only 4 missed hits in **CDG+(txt)**) is not significant. Overall, **CDG+(txt)** is 33.2% better than DKRL (CNN) in terms of the weighted-sum performance over **N-h**, **N-t** and **N-ht** together (i.e., total in Table 8). These results demonstrate the strong capability of **CDG+** in dealing with zero-shot problems in knowledge graph learning.

Table 8: Zero-Shot Learning on FB20k (H@10)

method	N-h	N-t	N-ht	total
CBOW [23]	27.1	21.7	67.2	24.6
DKRL (CNN) [23]	31.2	26.1	<b>72.5</b>	29.5
<b>CDG+(txt)</b>	<b>40.8</b>	<b>36.6</b>	69.8	<b>39.3</b>

The column of “total” has the weighted sum of H@10 over the three cases **N-h**, **N-t** and **N-ht**. The best performance under each metric is **bold**. H@10 values are in percent.

### 7.3 Representation Distribution

Fig. 7: Embeddings from **CDG** on DGI

We compare the embeddings learned from **CDG** and ComplEx on the DGI dataset, as ComplEx is very strong baseline according to Table 5. We use t-SNE method [13] to project the embeddings into 2-dimension space. Figure 7 presents the embeddings of drugs and genes learned from **CDG** in 2D space. Figure 8 presents the embeddings of the real vectors of drug and genes learned from ComplEx. The projected embeddings of imaginary vectors are very similar to that in Figure 8

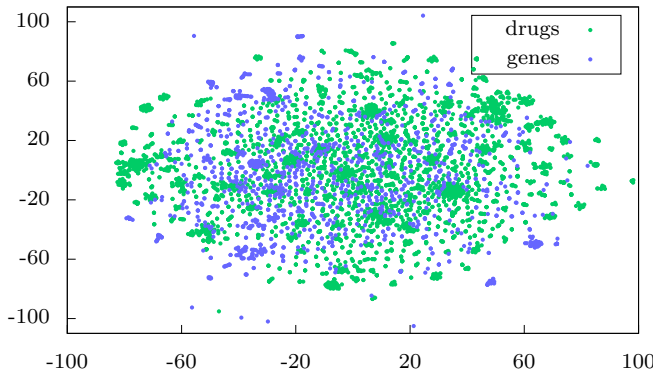


Fig. 8: Embeddings from ComplEx (Real Vectors) on DGI

so we don't present them here. Please note that in these two figures, a small Euclidean distance between a drug and a gene does not necessarily mean that the drug and gene tend to interact due to the ways the interactions are calculated in **CDC** (i.e., through CNN) and in **ComplEx** (i.e., through bilinear scoring).

In Figure 7, the drugs and genes are well separated by **CDC**, and there are some tight clusters among drugs and genes, respectively. However, in Figure 8, the drugs and genes are all mixed, and the clustering structure is less clear. We checked several clusters in Figure 7. Most of the drugs in drug cluster 1 in Figure 7 (i.e.,  $C_1^d$ ) are anti-inflammatory drugs (e.g., betamethasone, dexamethasone, fluorometholone, hydrocortamate and prednisolone), and belong to drug class corticosteroid and glucocorticoid. Most of the drugs in drug cluster 2 (i.e.,  $C_2^d$ ) are used to treat anxiety, tension, depression and insomnia (e.g., diazepam, meprobamate, methyprylon, temazepam and zaleplon). Most of the drugs in drug cluster 5 (i.e.,  $C_5^d$ ) are used to treat allergy symptoms and allergic rhinitis (e.g., azelastine, cetirizine, clemastine, dimethindene and triprolidine). There are also some tight gene clusters. For example, in gene cluster 1 (i.e.,  $C_1^g$ ) in Figure 7, almost all the genes are from gene group NADH:ubiquinone oxidoreductase core subunits (NDUF, MT-ND) (e.g., MT-ND5, MT-ND6, NDUFB9, NDUFV1 and NDUFS4). In gene cluster 5 (i.e.,  $C_5^g$ ), almost all the genes are from gene group Potassium voltage-gated channels (e.g., KCNQ5, KCNH6, KCNA2). Since drugs from a same drug class tend to be similar in terms of their chemical structures and/or their interactions with protein pathways, and genes from a same gene family tend to interact with similar drugs, the clustering structures among the drug and gene embeddings from **CDC** demonstrate that **CDC** is able to learn the entity relations that conform to knowledge.

#### 7.4 Case Study

Table 9 presents some examples from head prediction (**N-h**) and tail prediction (**N-t**) that **CDC** was able to correctly rank among top 10 in the corresponding testing lists, but **ComplEx** was not. The examples represented in Table 9 do not involve either rare drugs or rare side effects. Actually, they correspond to average

Table 9: Examples of **CDC** Prediction on DDI Dataset

	drug 1	drug 2	side effects
head prediction	fluconazole	metformin	enuresis
	guaifenesin	telithromycin	respiratory alkalosis
	amlodipine	sumatriptan	breast disorder
	voltaren	a-methapred	cystitis interstitial
	furosemide	rofecoxib	ingrowing nail
tail prediction	bupropion	acetaminophen	keratoconjunctivitis sicca
	cyclobenzaprine	ibuprofen	epicondylitis
	amitriptyline	carbamazepine	trigger finger
	clonazepam	gabapentin	enuresis
	diazepam	primidone	bunion

drug and side effects in the dataset. Thus, Table 9 shows that **CDC** is able to better prioritize true relations compared to ComplEx.

## 8 Conclusion and Future Work

In this paper, we developed a CNN-based dual-chain model (**CDC**) for knowledge graph learning. In **CDC**, two learning chains are constructed, one learning from the  $(h, r, t)$  triplet embeddings via a CNN and the following layers, the other learning from a sparsified version of the triplet embeddings via exactly same architectures as in the first chain. Our experimental results demonstrate that this CNN based method for triplet embedding learning, together with the dual-chain structure, is able to achieve or outperform the state-of-the-art results on graph learning. We also extended **CDC** to incorporate textual information (entity descriptions) into **CDC+**. Embeddings from descriptions are also learned via CNN and structure attention for the entities, in addition to the embeddings learned from knowledge graph structures. The two types of embeddings are both used to predict entities in **CDC+**. Therefore, **CDC+** is able to work for new entities that are not available during model training (i.e., zero-shot problem). Our experimental results demonstrate that **CDC+** outperforms other methods that are also able to handle zero-shot problems. In the future research, we will also incorporate the path and community information from the knowledge graph structures, in addition to textual information on entities, to further improve learning performance. We will also consider using the textual information of the entities along a path or within a community. We will also try and apply such methods in more impactful applications such as disease-gene association graph, etc.

## References

1. Bollacker K, Evans C, Paritosh P, Sturge T, Taylor J (2008) Freebase: a collaboratively created graph database for structuring human knowledge. In: Proceedings of the 2008 ACM SIGMOD international conference on Management of data, AcM, pp 1247–1250

2. Bordes A, Usunier N, Garcia-Duran A, Weston J, Yakhnenko O (2013) Translating embeddings for modeling multi-relational data. In: Advances in neural information processing systems, pp 2787–2795
3. Cotto KC, Wagner AH, Feng YY, Kiwala S, Coffman AC, Spies G, Wollam A, Spies NC, Griffith OL, Griffith M (2017) Dgidb 3.0: a redesign and expansion of the drug–gene interaction database. *Nucleic acids research* 46(D1):D1068–D1073
4. Dettmers T, Minervini P, Stenetorp P, Riedel S (2018) Convolutional 2d knowledge graph embeddings. In: Proceedings of the Thirty-Second AAAI Conference on Artificial Intelligence, (AAAI-18), the 30th innovative Applications of Artificial Intelligence (IAAI-18), and the 8th AAAI Symposium on Educational Advances in Artificial Intelligence (EAAI-18), New Orleans, Louisiana, USA, February 2-7, 2018, pp 1811–1818
5. Glorot X, Bengio Y (2010) Understanding the difficulty of training deep feed-forward neural networks. In: Proceedings of the thirteenth international conference on artificial intelligence and statistics, pp 249–256
6. He S, Liu K, Ji G, Zhao J (2015) Learning to represent knowledge graphs with gaussian embedding. In: Proceedings of the 24th ACM International on Conference on Information and Knowledge Management, ACM, pp 623–632
7. Ji G, He S, Xu L, Liu K, Zhao J (2015) Knowledge graph embedding via dynamic mapping matrix. In: Proceedings of the 53rd Annual Meeting of the Association for Computational Linguistics and the 7th International Joint Conference on Natural Language Processing (Volume 1: Long Papers), vol 1, pp 687–696
8. Ji G, Liu K, He S, Zhao J (2016) Knowledge graph completion with adaptive sparse transfer matrix. In: Proceedings of the Thirtieth AAAI Conference on Artificial Intelligence, February 12-17, 2016, Phoenix, Arizona, USA., pp 985–991
9. Lacroix T, Usunier N, Obozinski G (2018) Canonical tensor decomposition for knowledge base completion. *arXiv preprint arXiv:180607297*
10. Lehmann J, Isele R, Jakob M, Jentzsch A, Kontokostas D, Mendes PN, Hellmann S, Morsey M, Van Kleef P, Auer S, et al. (2015) Dbpedia—a large-scale, multilingual knowledge base extracted from wikipedia. *Semantic Web* 6(2):167–195
11. Lin Y, Liu Z, Sun M, Liu Y, Zhu X (2015) Learning entity and relation embeddings for knowledge graph completion. In: Proceedings of the Twenty-Ninth AAAI Conference on Artificial Intelligence, January 25-30, 2015, Austin, Texas, USA., pp 2181–2187
12. Lin Z, Feng M, dos Santos CN, Yu M, Xiang B, Zhou B, Bengio Y (2017) A structured self-attentive sentence embedding. *CoRR* abs/1703.03130
13. Maaten Lvd, Hinton G (2008) Visualizing data using t-sne. *Journal of machine learning research* 9(Nov):2579–2605
14. Mahdisoltani F, Biega J, Suchanek FM (2015) YAGO3: A knowledge base from multilingual wikipedias. In: CIDR 2015, Seventh Biennial Conference on Innovative Data Systems Research, Asilomar, CA, USA, January 4-7, 2015, Online Proceedings
15. Miller GA, Beckwith R, Fellbaum C, Gross D, Miller KJ (1990) Introduction to wordnet: An on-line lexical database. *International journal of lexicography* 3(4):235–244

16. Nickel M, Rosasco L, Poggio TA (2016) Holographic embeddings of knowledge graphs. In: Proceedings of the Thirtieth AAAI Conference on Artificial Intelligence, February 12-17, 2016, Phoenix, Arizona, USA., pp 1955–1961
17. Niepert M, Ahmed M, Kutzkov K (2016) Learning convolutional neural networks for graphs. In: International conference on machine learning, pp 2014–2023
18. Pennington J, Socher R, Manning C (2014) Glove: Global vectors for word representation. In: Proceedings of the 2014 conference on empirical methods in natural language processing (EMNLP), pp 1532–1543
19. Schlichtkrull M, Kipf TN, Bloem P, van den Berg R, Titov I, Welling M (2018) Modeling relational data with graph convolutional networks. In: European Semantic Web Conference, Springer, pp 593–607
20. Tatonetti NP, Patrick PY, Daneshjou R, Altman RB (2012) Data-driven prediction of drug effects and interactions. *Science translational medicine* 4(125):125ra31–125ra31
21. Trouillon T, Welbl J, Riedel S, Gaussier É, Bouchard G (2016) Complex embeddings for simple link prediction. In: International Conference on Machine Learning, pp 2071–2080
22. Wang Z, Zhang J, Feng J, Chen Z (2014) Knowledge graph embedding by translating on hyperplanes. In: Proceedings of the Twenty-Eighth AAAI Conference on Artificial Intelligence, July 27 -31, 2014, Québec City, Québec, Canada., pp 1112–1119
23. Xiao H, Huang M, Meng L, Zhu X (2017) Ssp: Semantic space projection for knowledge graph embedding with text descriptions. In: AAAI, vol 17, pp 3104–3110
24. Xie R, Liu Z, Jia J, Luan H, Sun M (2016) Representation learning of knowledge graphs with entity descriptions. In: Proceedings of the Thirtieth AAAI Conference on Artificial Intelligence, February 12-17, 2016, Phoenix, Arizona, USA., pp 2659–2665
25. Yang B, Yih W, He X, Gao J, Deng L (2014) Embedding entities and relations for learning and inference in knowledge bases. CoRR abs/1412.6575

## A Appendix

### A.1 Data Augmentation and Reproducibility Issues with ConvE

The training and testing data used in the ConvE are constructed in a different way compared to the data used in **CDC** and also the data used in other baseline methods such as TransE, Distmult and Complex. In ConvE, before training the model, for each triplet with reversible relation  $(h, r_{rv}, t)$ , it adds a reversed triplet  $(t, r_{rv}, h)$  into the training, validation and testing sets, correspondingly. As a result, ConvE has benefited from this data augmentation to achieve better performance [9]. Moreover, the reversed triplets on the testing set give the model two chances to predict a same triplet correctly. Thus, it further over-estimate the performance. However, in our experiments and the experiments of the baseline methods, such data augmentation before training is not implemented. So it is not fair to compare the reported results of ConvE with the experimental results of our model and baseline methods. This is an issue that has been recognized by others<sup>2</sup>. It is noteworthy that, without data augmentation, **CDC** can still achieve similar or even better performance than ConvE on almost all the public datasets used in our experiments. It demonstrates that the CNN architecture used in our model is very competitive or even better compared to the CNN architecture used in ConvE.

We also find that the source code of ConvE published on Github<sup>3</sup> will cause memory explosion issues and thus we can not reproduce the reported results in ConvE. Our computers with 16GB RAM can not run their code through on FB15k-237, which is a small dataset used in their paper, while it only takes about 3.5GB to run our model. Because of this, we reimplement ConvE with Tensorflow and train it on FB15k. However, it produces much worse results compared with the results reported by ConvE. Consequently upon these facts, we don't use ConvE as baseline in our experiments.

### A.2 Experimental Setting

We implemented the algorithm in python with tensorflow ([www.tensorflow.org](http://www.tensorflow.org)).

On the WN18, FB15k, FB15k-237 and DDI datasets, the learning rate starts from 3e-3; on the YAGO3-10, FB14k and DGI datasets, the learning rate starts from 1e-3. We decreased the learning rate in each epoch with a rate 0.998 on all the datasets. We find the following hyper-parameters work well on the datasets: on dataset WN18, the dimension of entity and relationship embedding  $k$  as 200, the number of convolutional kernel  $n_c$  as 64, the dimension of the triplet representations, denoted as  $d_g$ , as 256, the drop-out rate  $p$  as 0.2, batch size as 5,000, the number of training epochs as 3,000, and label smoothing weight as 0.0. On dataset FB15k, the best performing parameters are as follows:  $k=200$ ,  $n_c=64$ ,  $d_g=256$ ,  $p=0.2$ , batch size=5,000, number of epochs=3,000 and label smoothing weight=0.0; On dataset FB15k-237, the best performing parameters are as follows:  $k=200$ ,  $n_c=64$ ,  $d_g=256$ ,  $p=0.2$ , batch size=2,000, number of epochs=2,000 and label smoothing weight=0.1. On dataset DDI, the best performing parameters are as follows:  $k=200$ ,  $n_c=64$ ,  $d_g=256$ ,  $p=0.2$ , batch size=300, number of epochs=1,000 and label smoothing weight=0.0. On dataset YAGO3-10, the best performing parameters are as follows:  $k=200$ ,  $n_c=64$ ,  $d_g=256$ ,  $p=0.2$ , batch size=30,000, number of epochs=2,000 and label smoothing weight=0.0. On dataset FB14k, the best performing parameters are as follows:  $k=100$ ,  $n_c=64$ ,  $d_g=256$ ,  $p=0.2$ , batch size=1,000, number of epochs=600 and label smoothing weight=0.0. On dataset DDI, the best performing parameters are as follows:  $k=200$ ,  $n_c=64$ ,  $d_g=256$ ,  $p=0.2$ , batch size=100, number of epochs=1,000 and label smoothing weight=0.0. In order to avoid overfitting, we regularized the embedding of relations and entities to have unit  $\ell_2$  norm. We will publish the source code upon the acceptance of this paper.

### A.3 Comparison between **CDC** and ConvE on experimental results

Table 10 presents the comparison between **CDC** and ConvE. The results of ConvE are cited from its paper. On almost all the datasets, without data augmentation, **CDC** can still achieve similar

<sup>2</sup> <https://github.com/TimDettmers/ConvE/issues/45>

<sup>3</sup> <https://github.com/TimDettmers/ConvE>

or even better performance than ConvE. It demonstrates that the CNN architecture used in CDC is very competitive or even better compared to the CNN architecture used in ConvE.

Table 10: Comparison between CDC and ConvE

method	WN18		FB15k		YAGO3-10		FB15k-237	
	MR	H@10	MR	H@10	MR	H@10	MR	H@10
ConvE	374	95.6	51	83.1	1,676	62.0	244	50.1
CDC	380	94.9	73	83.3	2,061	62.9	267	46.2

H@10 values are in percent.